The British Journal of Radiology, *71*, (1998) 200–209

The practical peak voltage of diagnostic X-ray generators

[1]H M KRAMER, [1]H-J SELBACH and [2]W J ILES

[1]*Physikalisch-Technische Bundesanstalt, 38116 Braunschweig, Germany, and* [2]*National Radiological Protection Board, Chilton, Didcot, Oxon OX11 ORQ, UK*

Abstract. A new quantity termed the "practical peak voltage" is proposed. This quantity is derived by equating the low level contrast in an exposure made with an X-ray tube connected to a generator delivering any arbitrary wave form, to the contrast produced by the same X-ray tube connected to a constant potential generator. Out of the great number of possible contrast configurations one is selected as being suitable for diagnostic radiology. By means of an eigenvalue problem a direct link is established between the electrical quantity X-ray tube voltage and the practical peak voltage which was initially defined through the properties of the X-ray field. It is shown that the spread in total X-ray tube filtration as encountered in medical diagnostic radiology can influence the result of a measurement of the practical peak voltage only marginally.

Introduction

As part of the work of sub-committee 62C of the International Electrotechnical Commission (IEC), a project [1] is under way with the objective of specifying requirements for the performance characteristics of instruments for the non-invasive measurement of X-ray tube voltage in diagnostic radiology. One central prerequisite for specifying such requirements is that there is a definition of the quantity to be measured. Usually, the "peak voltage" is of interest, often referred to as kV_p. But, what is this peak voltage? Is it the maximum, the arithmetic mean or any other mean of all peak voltages or even something else? Until now this question has not been satisfactorily answered.

There are no published results on how the peak voltage as measured with most of the existing non-invasive instruments is associated with image properties. If, for instance, radiographs are produced from a high frequency, converter type generator and a two-pulse generator, both operating at the same measured value of the peak voltage, it is almost certain that the contrast in the radiographs from the two-pulse generator will be the higher.

Differences obtained with different instruments for the measurement of the X-ray tube voltage may be attributed to a poor calibration of one or more of the instruments involved. Whilst the question of the quality of the calibration inevitably plays an important role, it must be appreciated that the vagueness of the term peak voltage is also a contributory factor.

This paper proposes a new quantity termed the "practical peak voltage". This quantity is based on the concept that the radiation generated by a high voltage of any waveform produces the same contrast as radiation generated by an "equivalent" constant potential. The constant potential producing the same contrast for a specified contrast configuration and specified X-ray tube properties as the waveform under test is the "practical peak voltage". The idea of defining the peak voltage by means of the properties of the radiograph was put forward many years ago by Ardran and Crooks with the penetrameter [2]. Recently, the idea of defining the peak voltage via the contrast of the radiograph has been revived [3].

In the present paper, this idea is further developed. As a first step, a set of parameters is laid down leading to an unambiguous definition of a physical quantity appropriate for the measurement of peak voltage in radiographic investigations. The computational methods employed to quantify this concept are described and an account is given of the results obtained so far. In the second step, this concept is generalized so that it is applicable not just to the particular X-ray tube characteristics selected but to any equipment used in diagnostic radiology apart from mammography, which will be dealt with in a different study. An outline is given of the essential constructional characteristics of non-invasive high voltage measuring devices. To avoid a possible inhibition of technical developments the paper refrains from formulating requirements on the specifications of such instruments.

Received 14 October 1996 and in final form 17 June 1997, accepted 11 August 1997.

Published with permission of the National Radiological Protection Board.

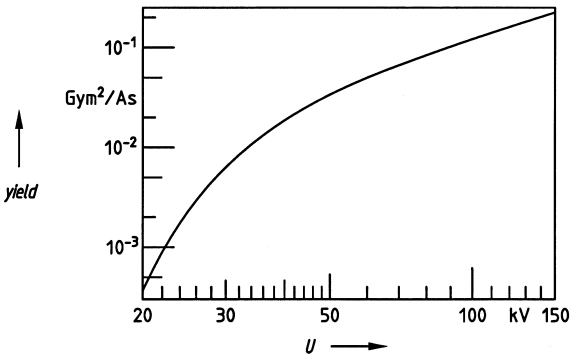

Figure 1. Diagram of the air kerma yield of an X-ray tube with 12° anode angle and total filtration of 2.5 mm Al as calculated according to Iles [4].

Determination of contrast-equivalent X-ray tube voltages from the contrast

The X-ray spectrum produced during an exposure time, t_e, by an X-ray tube supplied with a non-constant potential was approximated by superimposing a finite number of X-ray spectra, each corresponding to a constant potential. The weighting factor entered into this superposition for a spectrum of a given value of the constant potential U_i was proportional to the fraction of the time t_e in which the non-constant potential has a value in the interval $[U_i - \Delta U/2, U_i + \Delta U/2]$, where ΔU is a small voltage interval of fixed magnitude. The n spectra associated with the constant potentials $U_i = U_0 + i\Delta U$, $i = 0, n$ were calculated by a method published previously [4]. ΔU was chosen to be 1 kV and spectra for X-ray tube potentials ranging from 20 kV to 150 kV were calculated. In agreement with references [1] and [5] the following X-ray tube properties were chosen: a tungsten (W) anode, 12° anode angle, and 2.5 mm aluminium total beam filtration. Each spectrum was normalized so that the air kerma calculated from the spectral distribution was proportional to the yield from an X-ray tube with the above specifications. The yield curve is shown in Figure 1.

The present study covered a total of 75 different waveforms collected from all generator types presently available: one-, two-, six- and twelve-pulse, high frequency, converter-type and tetrode-type generators. Although this study is not applicable to the high voltage region used in mammography, 15 waveforms from mammography generators were included. In these 15 cases the value of the high voltage was normalized to a value typical of conventional X-ray diagnostics, *e.g.* 80 kV. A selection of four out of 75 waveforms is shown in Figure 2. Figure 3 is a histogram showing, for the four waveforms of Figure 2, the frequency distribution of occurrence of a voltage value in the interval $[U_i - \Delta U/2, U_i + \Delta U/2]$. Finally, in Figure 4, the corresponding four X-ray spectra are shown as derived from the superposition according to the frequencies in Figure 3.

For eight different contrast configurations, the contrast C_K defined as the ratio of air kerma

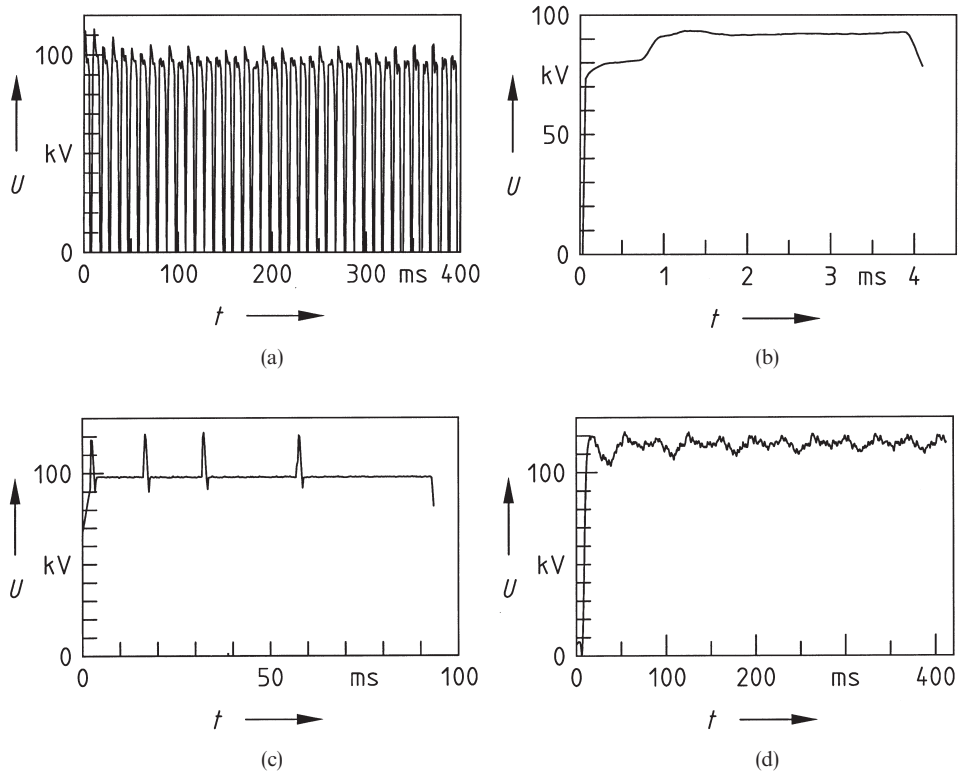

Figure 2. A selection of four examples out of the total of 75 waveforms considered in this study. (a) Two-pulse generator; (b) converter generator; (c) tetrode generator; (d) converter generator.

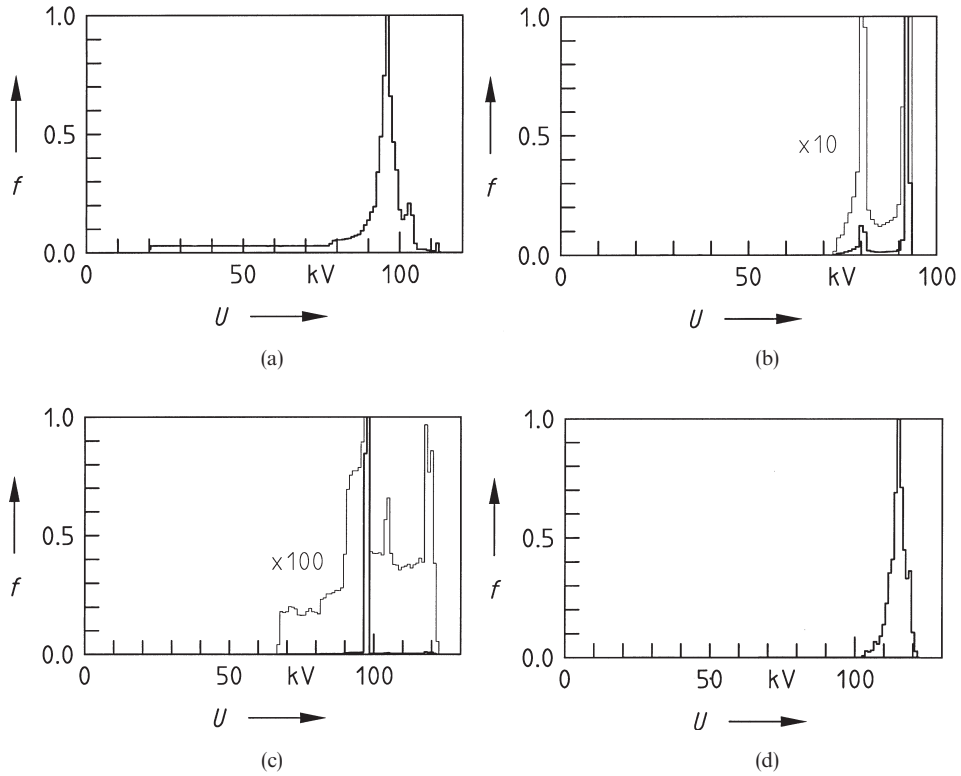

Figure 3. The frequency distribution with which a voltage in the interval $[U_i - \Delta U/2, U_i + \Delta U/2]$ occurs for the waveforms of Figures 2a to d as in Figure 2.

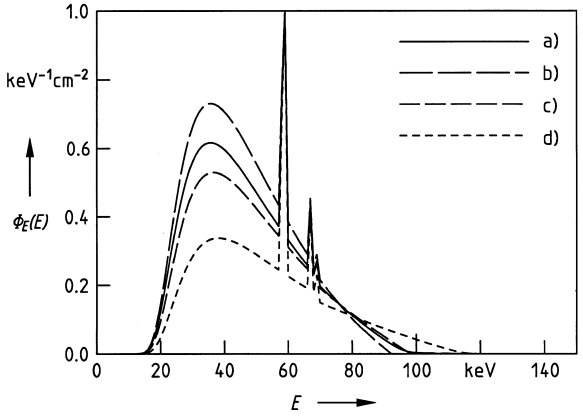

Figure 4. The four X-ray spectra associated with the four waveforms of Figure 2a to d as in Figure 2.

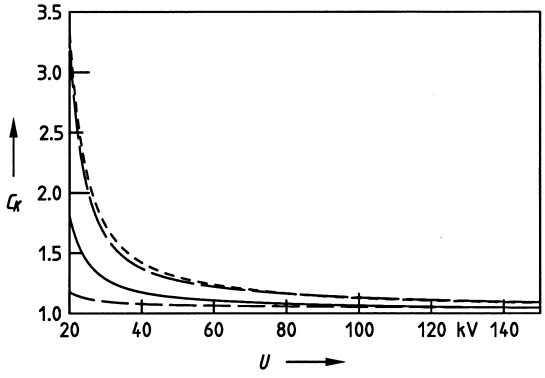

Figure 5. Curves with which the contrast as defined in Equation (1) is converted into the contrast-equivalent peak voltage: 10 cm PMMA phantom. The four curves relate to the contrast materials 0.5 mm Al (——), 1.0 mm Al (— —), 2.0 mm PMMA (– – –), 0.01 mm Pb (----).

behind the blank phantom and behind the phantom plus contrast material was calculated for each of the 75 waveforms according to:

$$C_K = \frac{\sum_{i=1}^{n} E_i \mu_{tr}(E_i) \phi_E(E_i) e^{-\mu_P(E_i) d_P}}{\sum_{i=1}^{n} E_i \mu_{tr}(E_i) \phi_E(E_i) e^{-(\mu_P(E_i) d_P + \mu_C(E_i) d_C)}} \quad (1)$$

where E_i is the photon energy of the interval i, μ_{tr} is the energy transfer coefficient for air, $\phi_E(E_i)$ is the photon fluence of the incoming radiation differentiated with respect to photon energy, μ_P, μ_C are the linear attenuation coefficient of phantom and contrast material, respectively, d_P, d_C are the thickness of phantom and of contrast material, respectively.

Two polymethyl-methacrylate (PMMA) phantoms 10 cm and 20 cm thick were combined with four contrast materials: 2 mm PMMA, 0.5 and 1 mm Al and 0.01 mm lead (Pb). All of these eight contrast configurations are characterized by $\mu_P d_P \gg \mu_C d_C$ which implies that the introduction of the contrast material is accompanied by only marginal changes in the spectrum behind the phantom.

Equation (1) was applied both to the spectra corresponding to constant potentials and to the spectra associated with the non-constant potentials. The latter were obtained by superposition of spectra as described above. Results for the spectra associated with the constant potentials are shown

Table 1. Contrast-equivalent voltages for the four examples (a) to (d) of the waveform of Figures 2 to 4

Contrast configuration	Contrast-equivalent peak voltage in kV			
	(a)	(b)	(c)	(d)
10 PMMA, 0.5 Al	93.399	89.854	98.057	114.634
10 PMMA, 1.0 Al	93.440	89.860	98.061	114.637
10 PMMA, 2.0 PMMA	93.614	89.899	98.102	114.666
10 PMMA, 0.01 Pb	93.097	89.769	97.974	114.616
20 PMMA, 0.5 Al	94.250	90.011	98.179	114.708
20 PMMA, 1.0 Al	94.274	90.016	98.183	114.710
20 PMMA, 2.0 PMMA	94.514	90.080	98.255	114.752
20 PMMA, 0.1 Pb	93.490	89.809	97.986	114.686

in Figure 5 for the 10 cm PMMA phantom. The corresponding curves for the 20 cm PMMA phantom are quite similar. These curves were used to convert the value of contrast obtained for a given combination of spectrum and contrast configuration into a value of the constant potential. Depending on the contrast configuration, the conversion functions differ significantly from each other. It will, however, be shown that the results obtained for the contrast-equivalent peak voltage are only marginally influenced by the particular nature of the contrast configuration itself.

Also, by analogy with the contrast-equivalent voltage, an attenuation-equivalent X-ray tube voltage was defined. Eight attenuation-value layers were considered; the first and second half-value layer and the first and second tenth-value layer of water and aluminium. Starting from the spectra associated with a constant potential, conversion curves for half-, quarter-, tenth- and hundredth-value layers for water and aluminium were obtained analogous to the data of Figure 5. For an X-ray spectrum associated with a non-constant potential, the various attenuation-value layer thicknesses were calculated and converted into a value of an attenuation-equivalent constant potential with the help of these conversion curves.

Influence of the contrast configuration

As an illustration, Table 1 presents the results of the contrast-equivalent X-ray tube voltage in units of kV for the four waveforms and the eight contrast configurations. In order to make the differences between the contrast configurations clearly visible the numerical values are given to a resolution of 1 V without claiming that this reflects the absolute accuracy. The greatest difference between the largest and the smallest value of the contrast-equivalent voltage is 1.4 kV. This occurs for the two-pulse generator as shown in column 2. For the other waveforms, the maximum difference is much smaller with typical values of a few hundred volts. The values in Table 1 demonstrate that even significant differences in the geometry as, for example, the 10 cm or the 20 cm PMMA phantom have a rather small effect on the value of the equivalent peak voltage. That there are small differences between the values of the equivalent voltages for the different configurations is only to be expected.

Table 2 presents the attenuation-equivalent voltages. Depending on the choice of the attenuation value layer a good correlation is found with contrast-equivalent peak voltages.

It is desirable that, with the exception of mammography, a single configuration be recommended as the reference for the whole X-ray region. Therefore, it is necessary to select one of the eight contrast configurations. It is reasonable to exclude the 20 cm PMMA configurations. This thickness would be unrealistic for both the lower and the upper levels of the X-ray tube voltages used in practice. At the lower end of the X-ray tube voltages, say 40 kV, it is unlikely that a radiograph through 20 cm of tissue would be made. At the higher end of the range of the X-ray tube voltages, radiographs of the chest are taken through 10 cm of tissue rather than 20 cm.

The contrast material lead is characterized by the disadvantage of having its K-absorption edge in the photon energy region of interest. This puts lead into an "outsider role" with respect to the other contrast materials. The remaining three

Table 2. Attenuation-equivalent voltages for the four examples (a) to (d) of the waveform of Figures 2 to 4

Attenuation layer	Attenuation-equivalent peak voltage in kV			
	(a)	(b)	(c)	(d)
H_2O-HVL	91.961	89.671	97.947	114.550
H_2O-QVL	92.287	89.710	97.972	114.571
H_2O-TVL	92.628	89.754	98.000	114.594
H_2O-HuVL	93.248	89.850	98.069	114.642
Al-HVL	92.154	89.688	97.954	114.559
Al-QVL	92.678	89.751	97.991	114.591
Al-TVL	93.201	89.827	98.041	114.627
Al-HuVL	94.086	90.014	98.184	114.705

HVL, half-value layer; QVL, quarter-value layer; TVL, tenth-value layer; HuVL, hundredth-value layer.

configurations are very close to each other with differences between them of the order of a few tens of volts. From practical considerations one would tend to exclude the 0.5 mm Al and the 2 mm PMMA. At higher X-ray tube voltages, the contrast (*cf*. Figure 5) drops in both cases to a value of about 1.05, and also the slope of the curve is rather small for X-ray tube voltages above about 120 kV. The latter point could lead to problems when the models are experimentally verified.

The practical peak voltage

From the above considerations, the configuration of 1 mm Al contrast on a 10 cm PMMA phantom is chosen as the reference. It is suggested to name the X-ray tube voltage defined by means of this contrast configuration the "practical peak voltage". By analogy with electron dosimetry where the "practical range" of electrons is defined by a measurement prescription, the "practical peak voltage" makes no claim to give a complete description of all physical processes involved. However, it represents a sufficiently stable basis for numerous operational decisions which have to be met in practice.

The histograms in Figure 6 show the frequency distribution of the differences between the practical peak voltage as the reference quantity and other contrast-equivalent peak voltages (a) and between the practical peak voltage and attenuation-equivalent peak voltages (b). In Figure 6a the influence of the phantom thickness is illustrated. In 52 cases out of the total 75 waveforms, the difference is less than 100 V, the maximum difference being 920 V. The larger differences are associated with the two-pulse generators. If this type of generator is disregarded, the maximum difference is reduced to 350 V.

From the X-ray tube voltages derived from the various attenuation-value layers, the aluminium tenth-value layer correlates best with the practical peak voltage. This was suggested already by the results presented in Table 2. Figure 6b gives the frequency distribution for the difference between the practical peak voltage and attenuation-equivalent voltage for the Al tenth-value layer for all 75 waveforms. In no case a difference in excess of 330 V occurs. Excluding the one- and two-pulse generators the results are within a maximum difference of 90 V.

Determination of the practical peak voltage from a directly measured X-ray tube voltage

As already addressed in the introduction, there is a dependence of the value of the contrast-equivalent voltage on the total beam filtration.

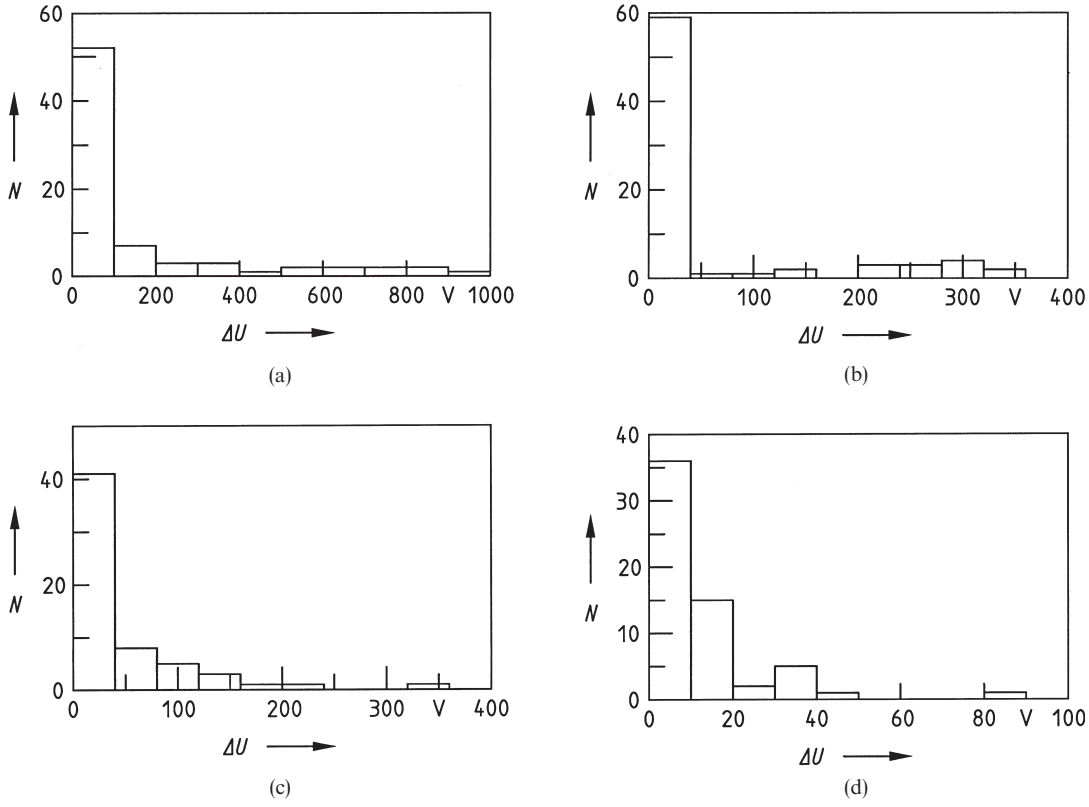

Figure 6. Histogram of differences between results for the 75 waveforms. Number of spectra *versus* (a) difference between practical peak voltage and the contrast-equivalent peak voltage for the 20 cm PMMA phantom with 1 mm Al contrast material, (b) difference between practical peak voltage and attenuation-equivalent peak voltage for the Al tenth-value layer. (c) and (d) as for (a) and (b) but without one- and two-pulse generators.

Normally, the total filtration is not accurately known. Even if it were known for a given X-ray tube at a given time, it can not be assumed that these properties remain unchanged for long periods due to processes like anode roughening etc. Such problems can be overcome by establishing a direct mathematical relation between the electrical quantity X-ray tube voltage and the contrast produced by the "reference" X-ray tube which was assumed to have a W-anode with an anode angle of 12° and 2.5 mm Al total filtration.

Such a relation is derived in the appendix. It leads to the definition of the practical peak voltage $\hat{U}$ in terms of the high voltage according to:

$$\hat{U} = \frac{\sum_{i=1}^{n} p(U_i) U_i w(W_i)}{\sum_{i=1}^{n} p(U_i) w(U_i)} \qquad (2)$$

where $p(U_i)$ is the probability of finding at any time during the exposure a potential in the interval $[U_i - \Delta U/2, U_i + \Delta U/2]$, with ΔU being a small voltage interval, and $w(U_i)$ is a weighting function which is approximated by two polynomials. For $20\ \text{kV} \leqslant U_i < 36\ \text{kV}$ one finds:

$$w(U_i) = \exp\{-8.646855 \times 10^{-3} U_i^2 + 0.8170361 U_i - 23.27793\} \qquad (3a)$$

and for $36\ \text{kV} \leqslant U_i \leqslant 150\ \text{kV}$ one finds:

$$w(U_i) = 4.310644 \times 10^{-10} U_i^4 - 1.662009 \times 10^{-7} U_i^3 + 2.30819 \times 10^{-5} U_i^2 + 1.03082 \times 10^{-5} U_i - 1.747153 \times 10^{-2} \qquad (3b)$$

where U_i is in kV.

With the help of Figure 5 the above relation allows the prediction of the contrast of the reference configuration (1 mm Al on a 10 cm PMMA phantom and the "reference" X-ray tube connected to the generator under test) on the basis of nothing else but electrical measurements of the high voltage. The spectral properties of the X-ray field produced by the combination of reference tube and generator under test are, of course, implicitly contained. However, they no longer enter explicitly as was the case in Equation (1). This definition of the practical peak voltage has the advantage of being directly based on the electrical quantity high voltage and, hence, being formally detached from the contrast considerations of Equation (1).

Influence of the X-ray tube characteristics on the practical peak voltage

It needs to be discussed now, as to how far the initial choice of the properties of the reference X-ray tube (W-anode, 12° anode angle, 2.5 mm Al filtration) has an impact on the result in terms of contrast and contrast-equivalent voltage. For such a consideration it is useful to restrict the properties of the X-ray tubes to be considered to a range which is not normally exceeded in medical diagnostic radiology. For the purpose of the following discussion it will be assumed that the anode angle can vary between 6° and 18° and the total filtration between 1.5 and 3.5 mm Al.

First, it is obvious that the contrast in a given contrast configuration depends on the total filtration in the X-ray tube. However, this has hardly any impact on the value of the contrast-equivalent voltage. This is so, because the contrast curve (see Figure 5) is used twice: (a) for the constant potential supply and (b) for the non-constant potential supply. In this way the value of the contrast itself occurs only as an intermediate quantity and is essentially eliminated after completion of the whole cycle.

Nevertheless, the contrast does depend on the total filtration of the X-ray tube which happens to be connected to the generator to be tested. Without any restrictions to the extent of the total beam filtration, the concept of a contrast-equivalent voltage is not sufficiently stable. However, there are no medical diagnostic X-ray tubes with, for instance, 6 mm Cu filtration. If the concept is restricted to the range of X-ray tubes considered above, the differences in contrast become quite small.

For worst case assumptions this is illustrated in Figure 7 for the example of a film–screen combination with a relatively high gradient which was chosen to be 3.5. For the reference X-ray tube the continuous curve shows the optical density of such a film behind 10 cm PMMA + 1.0 mm Al when the exposure is made so that the optical density behind 10 cm PMMA alone is 2. The broken curve

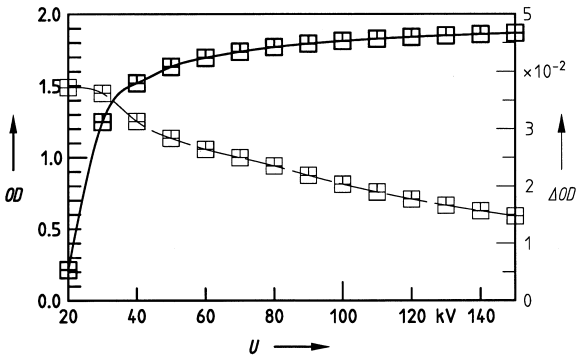

Figure 7. The optical density behind 10 cm PMMA + 1 mm Al assuming that the optical density behind 10 cm PMMA is 2 as function of X-ray tube potential (continuous curve and ordinate on the left hand side); difference in optical density when a X-ray tube with 18° anode angle and 1.5 mm Al is used instead of the reference to (broken curve and ordinate on the right hand side), for interpretation see text.

represents the difference in optical density behind the contrast material when a "soft" X-ray tube with 18° anode angle and 1.5 mm Al filtration is used, instead of the reference X-ray tube. Apart from the very low energy end at 40 kV and below all differences are below 0.03 OD. From the data presented by Hoeschen and He [6] it can be concluded that, in a direct comparison and under favourable circumstances, such differences can (just) be detected visually. If, however, a radiologist were to compare a radiograph made with the above soft X-ray tube with his visual anticipation of the radiograph made with the reference X-ray tube he would almost certainly not be able to detect the difference. This means that contrast differences caused by different inherent X-ray tube filtrations are essentially detectable only by means of measurements but hardly by visual inspection. Consequently, the practical peak voltage can be considered as a reliable quantity for predicting low-level contrast properties of a radiograph.

Routine measurement of the practical peak voltage

According to what has been presented so far, the value of the practical peak voltage can be determined experimentally either by contrast measurements or, more easily, by invasive voltage measurements. This leads to the questions whether (a) the practical voltage can also be measured with a non-invasive device and (b) if this can be done, what fundamental properties such a device should have. No principal obstacles have to be overcome to construct a pocket-calculator-size device. To permit sufficiently accurate measurements on systems having different values of beam filtration, both detectors of a non-invasive high-voltage meter must be heavily filtered. With such a device a measurement of the momentary value of a non-constant potential can be made with adequate accuracy irrespective of the precise extent of the total beam filtration. Most of the non-invasive high-voltage measuring devices currently available commercially function in fact in this way [7]. On no account should the detectors of a non-invasive high-voltage measuring device be constructed to resemble the contrast configuration. This would inevitably result in excessive sensitivity to the value of the beam filtration present in the system under test.

System inherent limitations of accuracy of about 100 V are due to the finite accuracy of the weighting function $w(U)$ and its approximation as given in Appendix 1. The overall accuracy of an instrument designed to measure the practical peak voltage will depend on the accuracy with which the voltage measurements are carried out. This is regardless of whether the kind of measurement is invasive or not. It is to be expected that an adequate accuracy can be realized only by digitizing the signal from the detector(s) at a rate which is high enough considering the generator frequencies. Once this has been performed, the digitized signal can either be fed to some kind of multichannel analyser with, say, 130 channels resulting in the distribution $p(U_i)$. The practical peak voltage is then calculated by means of Equations (2) and (3). Alternatively, the sums

$$\sum_{i=1}^{n} U_i w(U_i) \quad \text{and} \quad \sum_{i=1}^{n} w(U_i)$$

are calculated "on line" at the rate in which the momentary tube voltage U_i is digitized. In this case the practical peak voltage is obtained as the quotient of the two sums. In both cases the operation of such a device neither requires an *a priori* knowledge of the approximate range of the peak voltage nor of the generator type under test nor of the total beam filtration.

Summary and conclusions

A quantity for the measurement of the peak voltage on diagnostic X-ray generators is introduced which is termed "practical peak voltage". This quantity is derived from the contrast produced by a "reference" X-ray tube irradiating a 10 cm PMMA phantom covered partially with a piece of 1 mm Al as a contrast medium. For constant potentials, this contrast decreases monotonically with increasing voltage. Hence the contrast produced by an X-ray spectrum associated with any arbitrary waveform can always be unambiguously linked with a constant potential. As the spectral distribution of the radiation behind the phantom is modified only marginally by adding 1 mm of Al, the result of an experimental determination of the practical peak voltage is virtually independent of the energy dependence of the response of the detector employed for such a measurement. This implies that the practical peak voltage is directly related to the low level contrast both in radiography and in fluoroscopy.

The arbitrariness in the definition of the contrast configuration results in variations for the contrast-equivalent voltage of typically less than 1 kV. This is not an uncertainty, it indicates that different contrast configurations lead to results of the contrast-equivalent voltage which vary within 1 kV. By adopting one single contrast configuration these ambiguities are eliminated.

The above statement implies that the result of a determination of the contrast-equivalent peak voltage is virtually independent of small variations of the contrast geometry that inevitably come into play in experimental work due to the finite tolerances in the thickness of phantoms and contrast

materials. If, for example, the thickness of the aluminium contrast material on the 10 cm PMMA phantom is halved from 1.0 to 0.5 mm the results for the contrast-equivalent X-ray tube voltage are changed by 45 V at most for any of the 75 waveforms. If, for some reason, the thickness of the aluminium contrast material is not precisely known, it could for example be (1 ± 0.1) mm, the impact on the value of the practical peak voltage will be negligible.

By means of a mathematical transformation, the details of which are given in the appendix, it is demonstrated that the practical peak voltage, although initially defined via the contrast in a radiographic image, can also be defined on the basis of a direct measurement of the generator voltage. Determining the practical peak voltage according to either definition leads to differences not exceeding 100 V for any of the 75 waveforms. This figure is tolerable in view of the far greater simplicity of the calculation in the case of the definition based on the direct voltage measurement. It is also small enough to make the practical peak voltage a meaningful quantity. Apart from being much easier, the determination of the practical peak voltage from an electrical measurement has the advantage of being less sensitive to perturbing influences, such as for example, scattered radiation.

The practical peak voltage is not only useful for providing *a priori* information on the low-level contrast for X-rays produced by different generator types. It can also be used as a tool for setting the peak voltage of a generator with the objective of obtaining certain radiation qualitities as they are, *e.g.* defined in IEC Standard 1267 [8]. The procedure proposed there for adjusting the peak voltage is based on varying the peak voltage until the aluminium half-value layer assumes a certain value specific to the radiation quality in question. The results obtained in this study suggest that an adjustment in view of the aluminium tenth- instead of the half-value layer thickness (*cf* Figure 6b) would represent a link to the practical peak voltage which is even more direct.

Experimental investigations analogous to the calculations presented in this paper are nearly completed. Within the limits of uncertainty they confirm the theoretical findings [9].

It is to be expected that small pocket-calculator-size non-invasive instruments can be constructed which measure the practical peak voltage. The system inherent uncertainty of measurement of such instruments is of the order of 100 V. This implies that the actual uncertainty of measurement will be decided by the constructional qualities of the radiation detectors, the electronic hardware and software.

Finally, the limits of applicability of the proposed quantity should once more be emphasized. The results of this study refer to X-ray spectra without K- or L-edge filtration and with peak voltages in the range 30–150 kV. They are thus not applicable to spectra used in mammography. A similar study is under way in which the concept of a contrast-equivalent peak voltage will be extended to mammographic X-ray spectra generated by tungsten and molybdenum targets.

References

1. International Electrotechnical Commission. IEC 61676, Ed. 1: Medical electrical equipment — Dosimetric instruments for non-invasive measurements of X-ray tube voltage in diagnostic radiology. Geneva: IEC, 1996:62C/188/CD.
2. Ardran GM, Crooks HE. Penetrameter cassette calibration to 400 kV and effects of extra-focal radiation when measuring tube filtration. Br J Radiol 1978;51:29–34.
3. Kramer HM, Iles WJ, Selbach H-J. Was ist die Spitzenspannung bei diagnostischen Röntgenanlagen? In: Richter J, editor. Medizinische Physik. Würzburg: Deutsche Gesellschatt für Medizinische Physik, 1995:104–5.
4. Iles WJ. Computation of bremsstrahlung X-ray spectra over an energy range 15 keV to 300 keV, National Radiological Protection Board Report R204. London: HMSO, 1987.
5. International Electrotechnical Commission. International Standard IEC 601-1-3, Medical electrical equipment; part 1: General requirements for safety. 3. Collateral standard: General requirements for radiation protection in diagnostic X-ray equipment. Geneva: International Electrotechnical Commission, 1994.
6. Hoeschen D, He G. Visuelle Auswertung von Rasterbildern. PTB-Mitteilungen 1989;99:10–14.
7. Herrnsdorf L, Månsson LG, Strid K-G. Performance evaluation for in-beam quality control of X-ray equipment, Report MFT/Radfys 94:01. Gothenberg: Department of Radiation Physics, Gothenburg University, 1994.
8. International Electrotechnical Commission. International Standard IEC 1267, Medical diagnostic X-ray equipment—Radiation conditions for use in the determination of characteristics. Geneva: International Electrotechnical Commission, 1994.
9. Yue B, Kramer HM, Selbach H-J. In press.

Appendix 1

To establish a direct relation between the tube voltage and the practical peak voltage consider an exposure time t_e, and a waveform of the X-ray tube voltage which is characterized by the probability $p(U_i)$ of finding at any time during the exposure time t_e a potential in the interval $[U_i - \Delta U/2, U_i + \Delta U/2]$, where ΔU is a small voltage interval. The objective is to calculate directly the practical peak voltage $\hat{U}$ by means of a weighted sum over the voltages U_i occurring during

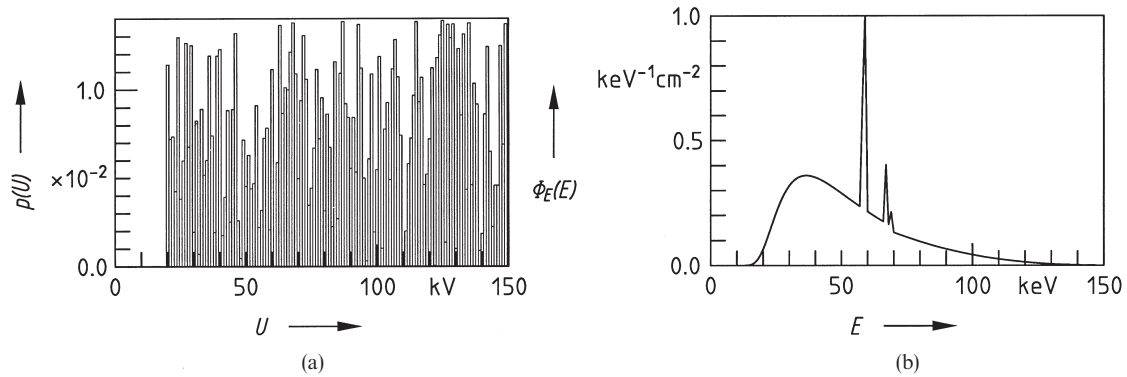

Figure 8. Example of a random distribution $p_j(U_i)$ obtained for one particular setting of the seed for the random number generator (a); corresponding X-ray spectrum (b).

the exposure time t_e, according to:

$$\hat{U}_j = \frac{\sum_{i=1}^{n} p_j(U_i) U_i w(U_i)}{\sum_{i=1}^{n} p_j(U_i) w(U_i)} \qquad \text{(A1)}$$

where $w(U_i)$ is the weight associated with X-ray tube voltage U_i and where the index j refers to the jth waveform. The denominator in Equation (A1) is introduced for the purpose of normalization. This equation can be rewritten to read:

$$\sum_{i=1}^{n} p_j(U_i)(U_i - \hat{U}_j) w(U_i) \equiv \mathbf{A} w(U_i) = \vec{\mathbf{0}} \qquad \text{(A2)}$$

where the symbol $\vec{\mathbf{0}}$ denotes a j-dimensional zero vector. Equation (A2) represents an eigenvalue problem. It has solutions only if the determinant of the matrix $\mathbf{A} - \lambda\mathbf{U}$ is zero, where $\mathbf{U}$ is a unit matrix and λ are the eigenvalues. The weighting factors $w(U_i)$ are the solution to the problem and they represent the eigenvectors. In principle, Equation (A2) can be solved in the form in which it is written if the number of different waveforms is equal to the number of X-ray tube voltage intervals n. However, such solutions may exhibit numerical instabilities and it is useful to multiply Equation (A2) from the left by the transposed matrix $\mathbf{A}^T$, which leads to

$$\mathbf{A}^T \mathbf{A} w(U_i) = \mathbf{A}^T \mathbf{A} \lambda \qquad \text{(A3)}$$

This procedure corresponds to a regression; it allows a number of waveforms $j > n$ to be used.

A number of different waveforms at least equal to the number of voltage intervals is required to solve Equation (A3). With values for the lowest and highest X-ray tube voltage of 20 and 150 kV and $\Delta U = 1$ kV, at least 131 distributions $p_j(U_i)$ are required for solving Equation (A3). In order not to create a self-consistent set of equations, the matrix $\mathbf{A}$ in Equation (A2) was made up of 200 different distributions $p_j(U_i)$ produced by a random number generator. Figure 8 gives an example of such a probability distribution together with the X-ray spectrum associated with it.

The transition to Equation (A3) furnishes a set of 131 equations. This set of equations was solved by means of a double-precision (about 16 significant digits) eigenvalue and eigenvector Fortran code. According to the nature of the problem, there are 131 eigenvalues and the same number of eigenvectors. It was found in practice that only the solution associated with the eigenvalue of the smallest absolute value was numerically robust. The solutions of $w(U_i)$ associated with eigenvalues of greater absolute values exhibited oscillations in sign of the elements. This is not acceptable as a solution. It implies that negative values of $\hat{U}$ can occur, which, of course, are physically meaningless. The above procedure was repeated several times with different seeds for the random number generator. In all cases, the best solution was associated with the eigenvalue with the smallest absolute value.

As an illustration, one such solution of $w(U)$ is presented in Figure 9. Within the accuracy of the drawing, the solutions $w(U)$ generated with different seeds of the random number generator are not distinguishable from the curve shown. The validity of the solutions $w(U)$ was tested for the 75 experimental waveforms. It should be emphasized that none of these 75 waveforms was used for

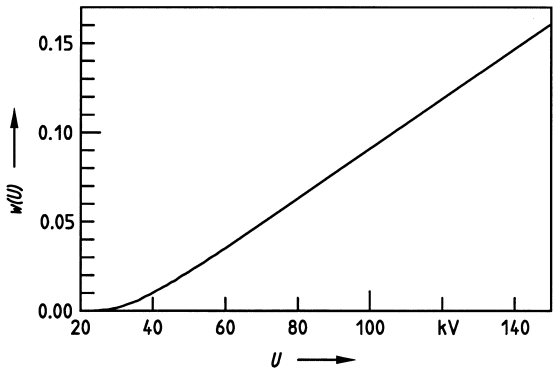

Figure 9. Graphic presentation of the eigenvector $w(U)$ associated with the eigenvalue of smallest absolute value. The eigenvectors associated with the higher eigenvalues exhibit oscillations.

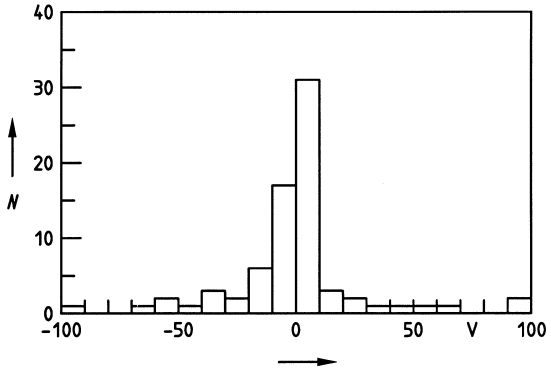

Figure 10. Number of spectra *versus* the differences in the practical high voltage for the 75 waveforms as calculated by Equations (A1) and (A2).

determining the solution vector $w(U_i)$. Figure 10 shows the differences between the results for the practical peak voltage calculated according to Equation (A1) with vectors $w(U_i)$ associated with different seeds of the random number generator.

All differences are smaller than 100 V. Although the histograms for the four random number generator seeds may look somewhat different, they essentially represent very similar distributions. The mean value of all distributions is very close to zero and never exceeds 1.5 V and the standard deviation of the four distributions is (27 ± 1) V.

Although the mathematical tools for deriving the practical peak voltage are quite straightforward, it cannot be denied that a substantial amount of data is required to carry out the complete contrast calculation. To facilitate the design of small non-invasive peak-voltage meters the algorithm is compressed by using a polynomial approximation for the eigenvectors $w(U_i)$. A sufficiently accurate approximation for $w(U_i)$ is obtained by dividing the total voltage range into two regions.

For $20\ \text{kV} \leqslant U_i < 36\ \text{kV}$ one finds:

$$w(U_i) = \exp\{-8.646855 \times 10^{-3} U_i^2 + 0.8170361 U_i - 23.27793\} \quad \text{(A4a)}$$

and for $36\ \text{kV} \leqslant U_i \leqslant 150\ \text{kV}$ one finds:

$$w(U_i) = 4.310644 \times 10^{-10} U_i^4 - 1.662009 \times 10^{-7} U_i^3 + 2.30819 \times 10^{-5} U_i^2 + 1.03082 \times 10^{-5} U_i - 1.747153 \times 10^{-2} \quad \text{(A4b)}$$

where U_i is in kV.

For a given probability distribution $p_j(U_i)$ the practical peak voltage can be calculated from an electrical measurement by inserting Equation (A4) into Equation (A1).